



Application of Nickel Calcite Nanoparticles in the Photodegradation of direct green 6 Dye

Santhosh A.M.¹, Yogendra K.^{1*}, Mahadevan K.M.², Mallikarjuna I.H.³ and Madhusudhana N.¹

¹Dept. of P.G. Studies and Research in Envi. Science, Kuvempu University, Jnana Sahyadri, Shankaraghatta, Shivamogga, Karnataka, India

²Department of P.G. Studies and Research in Chemistry, Kadur P.G Center, Kuvempu University, Kadur, Karnataka, India

³Department of Chemistry, Government Science College, Hassan, Karnataka, India

yogendraku@gmail.com

Available online at: www.isca.in, www.isca.me

Received 1st February 2018, revised 20th May 2018, accepted 18th June 2018

Abstract

Dyes are components associated with major water pollution and results in several health issues, so that alternative technologies are required in the treatment of dye effluent. In study mainly focused on photodegradation on Direct Green 6 (DG6) a textile dye by using synthesized Nickel Calcite (NiCaO₂) nanoparticles and these nanoparticles were prepared by economically viable method by using acetamide as a fuel. The characterization was done by X-ray diffraction (XRD), scanning electron microscope (SEM), Energy Dispersive X-ray (EDX), Brunauer Emmett-Teller surface area determination and UV-absorption spectroscopy. The results suggested that that, the band gap was found to be 3.3eV and also point zero charge was found to be 11.7, it is determined by pH drift method. Photocatalytic degradation was determined against DG6, with respect to parameters such as catalyst concentration, pH, dye concentration and in different conditions. From these experimental results we came to know that, the optimum catalyst concentration and pH was found to be 0.3g/100ml at pH 8. The maximum degradation was found to be 91.80%. Hence, the efficiency of photodegradation of DG6 dye by using NiCaO₂ nanoparticles was ascertained.

Keywords: Direct Green 6, NiCaO₂, Nanoparticles, Photodegradation.

Introduction

Textile effluents contributes a major contents of dye molecules, during dyeing process¹, which effects to the local water bodies, decrease in light penetration effects in photosynthesis² and these dye molecules are non-biodegradable, carcinogenic and mutagenic. Dyes are highly stable and complex aromatic structure¹. In the recent years, emerging technology leading heterogeneous photocatalytic degradation is easy way to colour from effluents due to their strong oxidation ability^{3,4}. In heterogeneous photocatalytic process, the UV/visible radiation cause photo-excitation in a semiconductor catalyst within the presence of oxygen.

Under these circumstances, photocatalytic degradation supported the powerful oxidizing species, either certain hydroxyl radicals or free holes are generated. Applying photocatalysts, organic pollutants are often fully mineralized by reacting with the oxidizers to create CO₂, water has mineral acids. The method is heterogeneous as a result of there is 2 active phases, solid and liquid^{5,6}.

The factor influencing photocatalytic degradation of dyes are, dye concentration, pH, and catalyst concentration, irradiation time and light intensity. In continuation of our work⁷⁻¹¹, we synthesized NiCaO₂ nanoparticles and studied for the colour removal of DG6 dye under natural sunlight. Hence, experiments

were conducted with NiCaO₂ nanoparticles by varying dye concentration, pH, catalyst loading and different conditions with respect to dark and UV conditions.

Materials and methods

Easily available dye in the market DG6 (λ_{\max} 592nm) was obtained from Mysore Paper Mill, Bhadravathi, Shivamogga, Karnataka (Figure-1). The chemicals Nickel Nitrate (Ni(NO₃)₂·6H₂O) (99% A.R.), Calcium Nitrate (Ca(NO₃)₂·4H₂O) (99%, A.R.), Acetamide (CH₃CONH₂) (99.5%), were procured from Hi-Media Chemicals, Mumbai. Through visible spectrophotometer (Elico, SL 177) the absorbance were recorded at λ_{\max} .

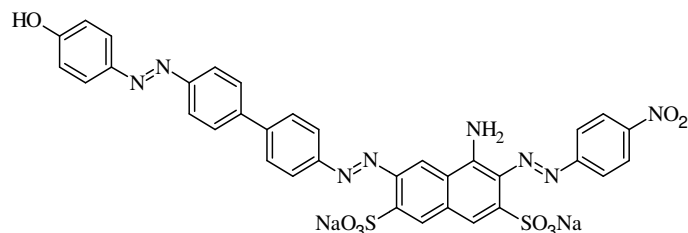


Figure-1: Chemical structure of DG6.

Synthesis of Nanoparticles: The nickel calcite nanoparticles have been synthesized by solution combustion method⁹, and

were subjected to photocatalytic degradation study against DG6 dye.



Characterization of Synthesized Nanoparticle: X-Ray Diffraction: The X-ray diffraction patterns of NiCaO₂ nanoparticles reveal that, the presence of Rhombo Hedral structure and the 2θ peaks were related to Nickel oxide, (37.29°, 43.30°, 62.87°, 75.40°, 79.33°) (JCPDS card No.01-089-3080) Calcite (23.13°, 29.48°, 39.48, 48.59°, 57.48°) (JCPDS card No.00-024-0027) and the XRD was performed by powder X-ray diffraction (Rigaku diffractometer) using Cu-Kα radiation (1.5406Å) in a θ-2θ configuration (Figure-2). According to the Debye Scherrer's formula:

$$D = K\lambda / \beta \cos\theta \quad (2)$$

In the present work, the powdered sample of newly synthesized NiCaO₂ nanoparticles were examined by XRD studies and found that, the found to be varied from 10nm to 24 nm and its average size was achieved on 19nm respectively.

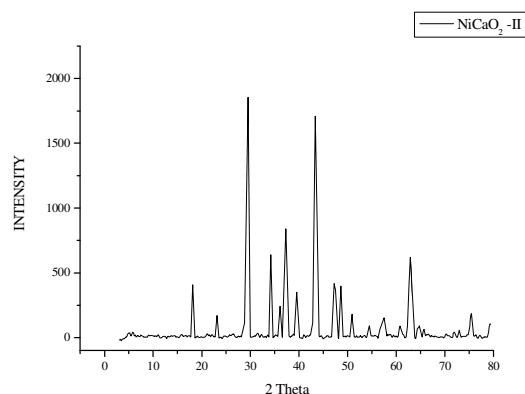


Figure-2: XRD of the synthesized NiCaO₂ (acetamide) Nanoparticles.

Scanning electron micrograph: The SEM pictures shows a cluster and foamy like structures. The enlarged image shows the uneven texture of the different nanoparticles, and also shows strong bonding of nanoparticles over one another (Figure-3)¹².

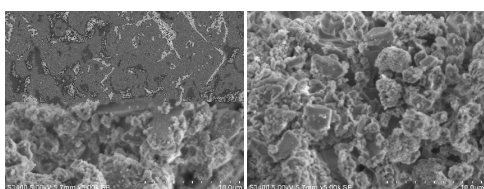


Figure-3: Scanning Electron Micrographs of synthesized NiCaO₂ (acetamide) Nanoparticles.

UV-Vis Absorption Spectroscopy: The optical absorption is a significant tool to get optical energy band gap of crystalline and amorphous materials. The elemental absorption corresponds to

the electron jumps from valence band to the conductivity band are often wont to verify the character and price of the optical band gap (OBG).

The spectrum reveals that, the NaCaO₂ nanoparticles absorption in the visible radiation with an above wavelength 400 nm. The OBG Eg is calculated from the relation:

$$(\alpha h\nu) = B(h\nu - E_g)^n \quad (3)$$

Where: 'hν' is the photon energy, 'B' is the constant and 'n' is the power factor and that takes 1/2, 2, 3/2 and 3 allowed direct, allowed indirect, forbidden direct and forbidden indirect transitions respectively. The OBG of the NaCaO₂ nanoparticle found to be 2.86eV.

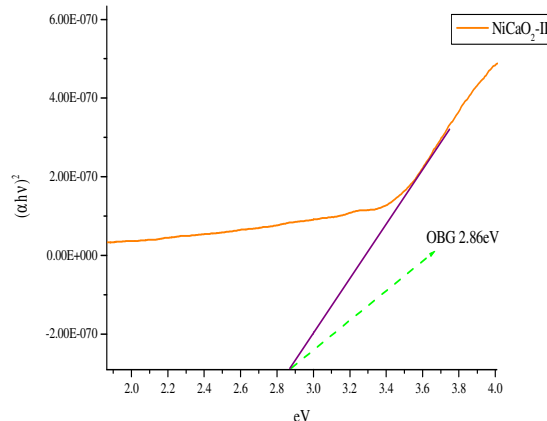


Figure-4: UV-absorption spectra of synthesized NiCaO₂ (acetamide) Nanoparticles.

Energy Dispersive X-ray: The confirmatory presence of elements was carried out using EDX spectrometer. The presence of Nickel, Calcium, Carbon and Oxygen signals of the NiCaO₂ nanoparticles. The vertical axis displays the amount of x-ray counts although, the horizontal axis displays energy in KeV (Figure-5). The weight and atomic percentage of Carbon, Oxygen, Calcium, and Nickel was found to be 20.56, 46.88, 17.85, 14.69 and 32.08, 54.88, 8.34, 4.69 these corresponds, the spectrum without impurities peaks⁹.

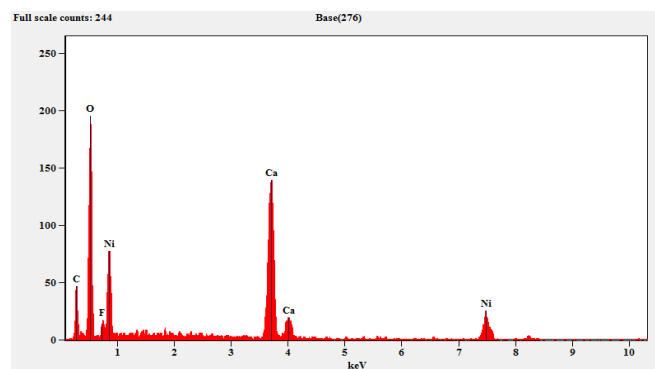


Figure-5: Energy Dispersive X-ray of synthesized NiCaO₂ (acetamide) Nanoparticles.

BET Surface area analysis: A specific surface area (SSA) of photocatalyst was measured at 77 K by Brunauer–Emmett–Teller (BET) nitrogen adsorption–desorption (NOVA-1000 version 3.70 Instrument). The BET surface area analysis, the SSA, pore volume and average pore diameter for NiCaO₂ nanoparticles shown in Table-1. This value is analogous to the other nanoparticles^{13,14}. The surface area obtained for NiCaO₂ nanoparticles was efficient to carry out the photocatalysis, which was directly proportional to the surface area available¹⁵.

Table-1: Surface properties of the nanoparticles.

Catalyst	Surface area	Pore volume	Average pore diameter
NiCaO ₂ (acetamide)	2.3778 m ² /g	0.00265 cc/g	44.578Å

Experimental Procedure: The experiments were conducted in presence of direct sunlight. Prepare known concentration of solution by dissolving 0.02g of DG6 dye in 1000ml double distilled water and decolourization was investigated in presence of NiCaO₂ nanoparticle at different catalyst dosages, pH levels and different experimental conditions. After the exposure, decolourization of the dye was recorded by visible spectrophotometer (Elico, SL 177) to know the optimum catalyst concentration. Hence, the experiments were repeats for different pH levels for the same standard dye solutions with the optimum concentration of catalyst.

$$D = \frac{A_0 - A_t}{A_0} \times 100$$

Where: A₀ is the initial absorbance of the dye solution, A_t is absorbance at time interval 't' i.e., after 120 min.

Results and discussion

Point of zero charge: Point of zero charge (PZC) or iso-electric point was the pH of the solution at which, the charge on the surface of the nanoparticles turns zero (neutral). The PZC of NiCaO₂ were carried out by pH drift method, 50ml of NaCl 0.01M were taken in 6 different beakers and bubbled it with Nitrogen gas to expel the dissolved CO₂ for few minutes at room temperature till it get a stable pH reading. To each one of the beakers was adjust between 2-12 pH by adding 0.1N NaOH and HCl and by adding 50mg of NiCaO₂ nanoparticles kept in room temperature until concurrent pH measured; this was kept for 92hrs for the stabilization of pH. The graph was plot against final pH v/s initial pH, point which crosses the curve of initial and final pH and plot the straight line is PZC. To understand the adsorption behaviour or photocatalysts affecting pH, PZC of NiCaO₂ nanoparticles was found to be 11.7 (Figure-6). Below this pH_(pzc) the surface becomes positive in nature and above this pH_(pzc) the surface is negative in nature. The pH of NiCaO₂ is below the pH_(pzc), which favours the degradation of DG6 and thus the suitable for photocatalysis¹⁵.

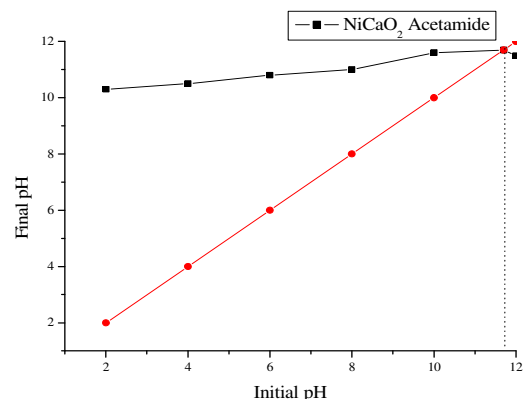
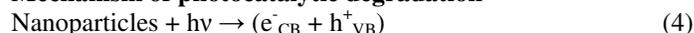


Figure-6: PZC of NiCaO₂ nanoparticles.

Mechanism of photocatalytic degradation



Step-1: When sunlight falls on the nanoparticles, it gets excited and the electrons gets transferred from valance band to conduction band.



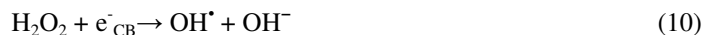
Step-2: It can reduce molecular oxygen and super oxide radicals were produced.



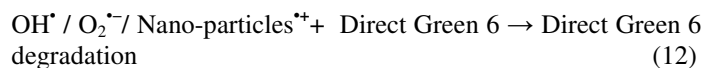
Step-3: The adsorbed molecular oxygen on the photocatalytic surface prevents the hole-electron pair recombination process⁸ and decrease photodegradation and this can be produced by hydrogen peroxide or organic peroxide in front of oxygen and organic molecule.



Step-4: From the other path Hydrogen peroxide can be generated.



Step-5: The powerful oxidizing agent hydroxyl radicals produced by the hydrogen peroxide.



Step-6: The produced hydroxyl radicals are more efficient in degrading the dye molecules.

Effect of catalyst loading: The effect of concentration NiCaO₂ photocatalyst on the photodegradation was examined over a range of 0.1 to 1g/100ml for DG6. The prepared nanoparticles have shows satisfactory results. The NiCaO₂ (acetamide) with the nanoparticle size 19 nm has shown 90.16 % degradation. Since, the photodegradation was very efficient at 0.3g/100ml in 120 minutes for NiCaO₂ nanoparticles concentration showed in (Figure-7) (Photo-1). The degradation increasing proportional to catalyst loading upto 0.3g/100ml since, more number of active sites are exposed, resulting dye molecule adsorb on the surface of the nanoparticles^{16,17} and further decrease (0.4g to 1g) in degradation due to more number of active sites present on the surface of the catalyst and block penetration of sunlight to the solution. The over loading of catalyst tends to the overcrowding, leads to turbidity of the solution and blocking the photons entering into the solution. Further, experiments were continued with same dosages¹⁸⁻²⁰.

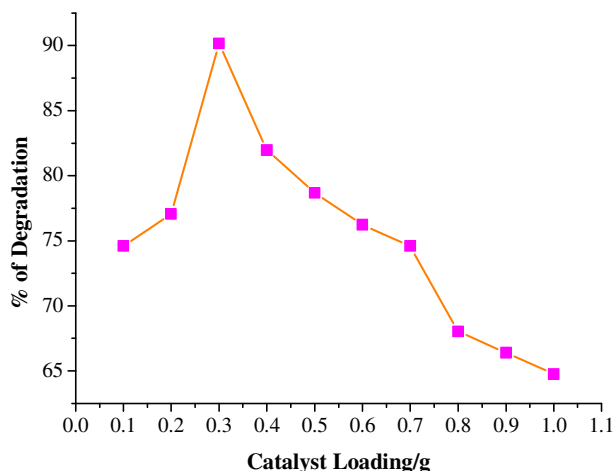


Figure-7: Effect of catalyst concentration on DG6 at 120 minutes [DG6=20 ppm, pH=7, NiCaO₂ (acetamide)].

Effect of pH: The effect of pH is the only factor depends on the degradation; the experiments were carried out at pH varying from 2 to 11. The percentage of degradation of DG6 for NiCaO₂ nanoparticles was obtained from 61.47% to 91.80% from pH 2 to 8, similarly the degradation decreases to 59.83% at pH 11 in

120 minutes for 0.3g/100ml. From the result we know that pH is affecting the efficiency of degradation (Figure-8) (Photo-2).

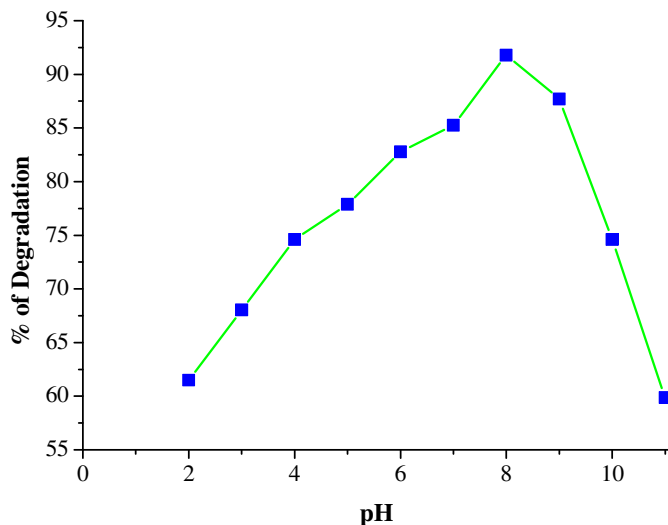


Figure-8: Effect of pH on DG6 at 120 minutes [DG6=20 ppm, NiCaO₂ (acetamide)].

The highest degradation was found at pH 8. However, the pH of the solution is increases the degradation also increases upto 8 and further decreases the degradation. Photocatalytic activity explains on the basis of PZC of the nanoparticle was found to be 11.7 (Figure-6). The below the pzc of the surface is positive in nature and above the pzc of the surface is negative in nature. The experimental results show that, the degradation was effectively in pH 8 due to the interaction between the dye and nanoparticles leads to generation of OH[•] in the alkaline medium and main oxidizing species OH[•] radicals are responsible for the photodegradation.

Above the pH 9 the degradation is decrease due to amphoteric nature of the catalyst and electrostatic repulsion between negatively charged dye molecules and the catalyst²¹⁻²³. Thus, the adsorption is mainly depends on the pH of the solution¹⁶.



Photo-1: Effect of catalyst concentration on DG6 at 120 minutes [DG6=20 ppm, pH=7, NiCaO₂ (acetamide)].



Photo-2: Effect of pH on DG6 at 120 minutes [DG6=20 ppm, NiCaO₂ (acetamide)].

Effect of initial dye concentration: The present work was carried out to study the effect of initial concentration of the dye by varying the DG6 concentration from 20, 30, 40, and 50 ppm respectively (Photo-3). The results obtained for NiCaO₂ is 91.80% for 20ppm, 87.70% for 30ppm, 79.50% for 40ppm and 54.09% for 50ppm respectively (Figure-9). As the dye concentration increases the capability of degradation decreases²⁴⁻²⁶ and the dye concentration increased the colour gets deeper, decrease the photons penetration to the solution, surface of the catalyst affected by the photons interception^{26,27} and this experiment clearly shows that, the interaction of dye and catalyst should be in optimum range²⁸.

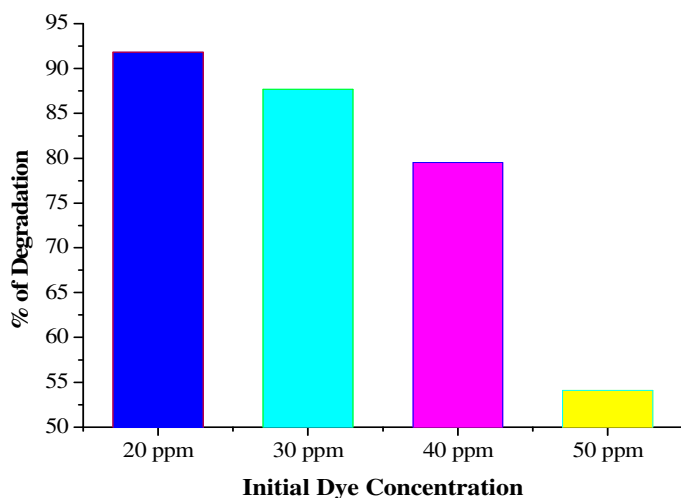


Figure-9: Effect of initial dye concentration on the photodegradation of DG6 [NiCaO₂ (acetamide) g/pH=0.3/8 and DG6= (20, 30, 40 and 50) ppm].



Photo-3: Effect of initial dye concentration on the photodegradation of DG6 [NiCaO₂ (acetamide) g/pH=0.3/8 and DG6= (20, 30, 40 and 50) ppm].

Effect of sunlight irradiation: The degradation of DG6 dye (20mg/L) were examined under 3 different conditions, i.e., through, dye/dark/catalyst, dye/UV/catalyst and dye/sunlight/catalyst for the catalyst. The degradation of the dye was found to be nil throughout the experiment when exposed to sunlight due to absence of catalyst.

The percentage of degradation was increased with increase in irradiation time, for dye/sunlight/NiCaO₂ showed 91.80%, for dye/dark/ NiCaO₂ 35.24% and for dye/UV/catalyst 73.77% was recorded (Figure-10). From this result we know that, the degradation efficient in sunlight is more when compared to UV and dark conditions (Photo-4)^{8,29,30}.

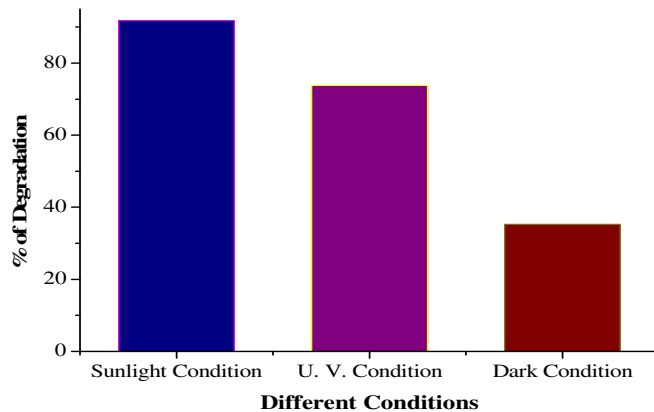


Figure-10: Effect of sunlight irradiation with respect to Dark and UV conditions on photodegradation of DG6 in 120 minutes.



Photo-4: Effect of sunlight irradiation with respect to Dark and UV conditions on photodegradation of DG6 in 120 minutes.

Conclusion

This study, mainly focused on the photodegradation of DG6 dye by NiCaO₂ nanoparticles. These nanoparticles were characterized by XRD, SEM, EDX, BET and UV-Vis reflectance. The pzc was found to be 11.7. These nanoparticles achieved maximum degradation (91.80%) at 0.3g/100ml for pH 8 in a very short span of time (120 min). For dark condition 35.24% and UV 73.77% were recorded. So here, the efficiency of NiCaO₂ nanoparticles were examined on DG6 and positive results were observed. Hence, NiCaO₂ nanoparticles can be effectively used in the process of photodegradation in a wider range in industries and environmental related issues.

References

1. Weldemariam Y. and Welderfael T. (2015). Photocatalytic Degradation of Methyl Orange by Ag-N Co-Doped ZnO Nanoparticles. *Chemistry and Materials Research*, 7(8), 40-49.
2. Elavarasi N. and Priya G.P. (2015). Decolourization of Methyl Orange Dye from Synthetic Waste water using Biosynthesized Iron Nanoparticles. *International Journal of Pharma and Bio Sciences*, 6(1), 423-430.
3. Chatchai P., Nosaka A.Y. and Nosaka Y. (2013). Photoelectrocatalytic performance of WO₃/BiVO₄ toward the dye degradation. *Electrochimica Acta*, 94, 314-319. doi.org/10.1016/j.electacta.2013.01.152.
4. Gopalappa H., Yogendra K., Mahadevan K.M. and Madhusudhana N. (2012). A comparative study on the solar photocatalytic degradation of Brilliant Red azo dye by CaO

- and CaMgO₂ nanoparticles. *International Journal of Science Research*, 1(2), 91-95.
- Malato S., Blanco J., Vidal A. and Richter C. (2002). Photocatalysis with solar energy at a pilot-plant scale: an overview. *Applied Catalysis B: Environmental*, 37, 1-15.
 - Pandey A., Singh P. and Iyengar L. (2007). Bacterial decolorization and degradation of azo dyes. *International Biodeterioration & Biodegradation*, 59(2), 73-84.
 - Madhusudhana N., Yogendra K., Mahadevan K.M. and Santhosh A.M. (2017). Synthesis and Application of MgZnSrO₃ Nano-Particle to the Photocatalytic Decolorization of Victoria Blue B Dye (VBB). *International Journal of Advance Research in Science and Engineering*, 6(8), 52-61.
 - Madhusudhan N., Yogendra K., Mahadevan K.M. and Kiran G.R. (2017). Synthesis and Application of MgZnSrO₃ Nano-particle for the Photocatalytic decolorization of Coralene Dark Red 2B Azo Dye (CDR 2B). *AGU International Journal of Science and Technology*, 5, 1-10.
 - Santhosh A.M., Yogendra K., Mahadevan K.M. and Madhusudhana N. (2017). Photodegradation of Congo Red azo dye, a Carcinogenic Textile dye by using synthesized Nickel Calcite Nanoparticles. *International Journal of Advance Research in Science and Engineering*, 6(7), 51-64.
 - Shilpa G., Yogendra K., Mahadevan K.M. and Madhusudhana N. (2017). Synthesis of ZnAl₂O₄ Nano-Particles and Its Application for Photo-Catalytic Decolorization of Model Azo Dye Acid Red 88 in Presence of Natural Sunlight. *IOSR Journal of Applied Chemistry*, 10(7), 35-41. DOI: 10.9790/5736-1007023541.
 - Kiran G.R., Yogendra K., Mahadevan K.M. and Madhusudhana N. (2017). Solar Photocatalytic decolorization of Direct blue 14 dye by using Synthesized SrO Nanoparticles. *International Journal of Advance Technology in Engineering and Science*, 5(7), 173-182.
 - Gurushantha K., Anantharaju K.S., Nagabhushana H., Sharma S.C., Vidya Y.S., Shivakumara C., Nagaswarupa H.P., Prashantha S.C. and Anilkumar M.R. (2015). Chemical Facile green fabrication of iron-doped cubic ZrO₂ nanoparticles by *Phyllanthus acidus*: Structural, photocatalytic and photoluminescent properties. *Journal of Molecular Catalysis A: Chemical*, 397, 36-47. doi:10.1016/2014.10.025.
 - Ye L.I.U., Qin M.L., Zhang L., Jia B.R., Cao Z.Q., Zhang D.Z. and Qu X.H. (2015). Solution combustion synthesis of Ni-Y₂O₃ nanocomposite powder. *Transactions of Nonferrous Metals Society of China*, 25(1), 129-136. doi: 10.1016/S1003-6326(15) 63587-7.
 - Yang T., Xia D., Chen G. and Chen Y. (2009). Influence of the surfactant and temperature on the morphology and physico-chemical properties of hydrothermally synthesized composite oxide BiVO₄. *Materials Chemistry and Physics*, 114, 69-72. doi:10.1016/j.matchemphys. 2008.08.005.
 - Kulkarni S.D., Kumbar S., Menon S.G., Choudhari K.S. and Santhosh C. (2016). Magnetically separable core-shell ZnFe₂O₄@ZnO nanoparticles for visible light photodegradation of methyl orange. *Materials Research Bulletin*, 77, 70-77. doi.org/10.1016/ j.materresbull. 2016.01.022.
 - Sobana N., Thirumalai K. and Swaminathan M. (2016). Kinetics of Solar Light Assisted Degradation of Direct Red 23 on Activated Carbon-loaded Zinc Oxide and Influence of Operational Parameters. *Canadian Chemical transactions*, 4(1), 77-89. doi.org/10.13179/canchemtrans. 2016.04.01.0258
 - Sangari N.U. and Velusamy P. (2016). Photocatalytic Decoloration Efficiencies of ZnO and TiO₂: A Comparative Study. *Journal of Environmental Science and Pollution Research*, 2(1), 42-45.
 - Bdewi S.F., Abdulrazaka A.M. and Aziz B.K. (2015). Catalytic Photodegradation of Methyl orange using MgO nanoparticles prepared by molten salt method. *Asian Transactions on Engineering*, 5(6), 1-5.
 - Subramani A.K., Byrappa K., Ananda S., Lokanatha Rai K.M., Ranganathaiah C. and Yoshimura M. (2007). Photocatalytic degradation of indigo carmine dye using TiO₂ impregnated activated carbon. *Bulletin of materials science*, 30, 37-41. doi:10.1007/s12034-007-0007-8.
 - Sakthivel S., Neppolian B., Shankar M.V., Arabindoo B., Palanichamy M. and Murugesan V. (2003). Solar photocatalytic degradation of azo dye: comparison of photocatalytic efficiency of ZnO and TiO₂. *Solar Energy Materials & Solar Cells*, 77, 65-82.
 - Turchi C.S. and Ollis D.F. (1990). Photocatalytic Degradation of Organic Water Contaminants: Mechanisms Involving Hydroxyl Radical Attack. *Journal of Catalysis*, 122, 178-192.
 - Guillard C., Lachheb H., Houas A., Ksibi M., Elaloui E. and Herrman J.M. (2003). Influence of chemical structure of dyes of pH and of inorganic salts on their photocatalytic degradation by TiO₂ Comparison of efficiency of powder and supported TiO₂. *Journal of Photochemistry and Photobiology A: Chemistry*, 158, 27-36. doi:10.1016/S1010-6030(03)00016-9
 - Mehta R. and Surana M. (2012). Comparative study of photo-degradation of dye Acid Orange-8 by Fenton reagent and Titanium Oxide- A review. *Der Pharma Chemica*, 4(1), 311-319.
 - Natarajan K., Natarajan T.S., Bajaj H.C. and Tyade R.J. (2011). Photocatalytic reactor based on UV-LED /TiO₂ coated quartz tube for degradation of dyes. *Chemical*

- Engineering Journal*, 178, 40-49. doi: 10.1016/j.cej.2011.10.007.
25. Neppolian B., Choi H.C., Sakthivel S., Arabindoo B. and Murugesan V. (2002). Solar light induced and TiO₂ assisted degradation of textile dye reactive blue. *Chemosphere*, 46(8), 1173-1181.
26. Habib A., Shahadat T., Bahadur N.M., Ismail I.M.I. and Mahmood A.J. (2013). Synthesis and characterization of ZnO-TiO₂ nanocomposites and their application as photocatalysts. *International Nano Letters*, 3(5), 1-8. doi:10.1186/2228-5326-3-5.
27. Chakrabarti S. and Dutta B.K. (2004). Photocatalytic degradation of model textile dyes in wastewater using ZnO as semiconductor catalyst. *Journal of Hazardous Materials B*, 112, 269-278. doi:10.1016/j.jhazmat.2004.05.013.
28. Raveendra R.S., Prashanth P.A., Krishna R.H., Bhagya N.P., Nagabhushana B.M., Naika H.R., Lingaraju K., Nagabhushana H. and Prasad B.D. (2014). Synthesis, structural characterization of nano ZnTiO₃ ceramic: An effective azo dye adsorbent and antibacterial agent. *Journal of Asian Ceramic Societies*, 2(4), 357-365. doi.org/10.1016/j.jascr.2014.07.008.
29. Movahedi M., Mahjoub A.R. and Darzi J.S. (2009). Photodegradation of Congo red in Aqueous Solution on ZnO as an Alternative Catalyst to TiO₂. *Journal of the Iranian Chemical Society*, 6(3), 570-577.
30. Santiago G.A., Mayen S.A., Delgado G.T., Perez C.R., Maldonado A. and Olvera-de-la M.L. (2010). Photocatalytic degradation of Methylene blue using undoped and Ag doped TiO₂ thin films deposited by a sol gel process: Effect of the ageing time of the starting solution and the film thickness. *Materials Science and Engineering B*, 174(1-3), 84-87. doi:10.1016/j.mseb.2010.03.009.